Research Square

Preprints are preliminary reports that have not undergone peer review.
They should not be considered conclusive, used to inform clinical practice,
or referenced by the media as validated information.

Mechanistic insights into genotoxicity caused by complex chemical mixtures in drinking water using effect-based assessment and Cell Painting

Aline Colonnello Montero
aline.colonnello.montero@slu.se
Swedish University of Agricultural Sciences
Malin Jarvius
Uppsala University
Jonne Rietdijk
Uppsala University
Maris Lapins
Uppsala University
Jordi Carreras-Puigvert
Uppsala University
Ola Spjuth
Uppsala University
Johan Lundqvist
Swedish University of Agricultural Sciences

Research Article

Keywords: Genotoxicity, Oxidative stress, Effect-based assessment, Cell Painting, Morphological profiles, Genotoxic mechanisms

Posted Date: September 29th, 2026

DOI: https://doi.org/10.21203/rs.3.rs-11077768/v1

License: This work is licensed under a Creative Commons Attribution 4.0 International License. Read Full License

Additional Declarations: Competing interest reported. J.L. is the founder and owner of BioCell Analytica Uppsala AB, a company providing effect-based testing services to the water sector. A.C.M. has been employed by the same company. All other authors declare that they have no known competing financial interests or personal relationships that could have appeared to influence the work reported in this paper.

Abstract

Background

In water quality, genotoxicity is a critical safety endpoint as genotoxicants can damage DNA directly or indirectly. Genotoxic activity has previously been detected in source water from lake Mälaren, throughout the conventional treatment process, and in drinking water at the Görväln drinking water treatment plant, with the highest activity during autumn-winter. Because genotoxicity poses a serious risk to human health, it is essential to investigate whether the underlying genotoxicity arises from direct and/or indirect mechanisms.

Aim

In this study we combined the micronucleus and oxidative stress bioassays with morphological profiling using Cell Painting with the aim of increasing our understanding of the mechanisms causing the genotoxicity.

Methods

For this purpose, we assessed the presence of genotoxicity in raw, sand-filtration and drinking water and the removal efficiency of the pilot treatment process with granular activated carbon filtration using effect-based assessment and morphology profiling.

Results

Data showed that samples from the conventional treatment process were genotoxic and induced oxidative stress, whereas the pilot treatment process removed genotoxic activity and reduced oxidative stress levels. Moreover, all samples induced morphological perturbations, but only genotoxic samples decreased nuclear area and increased granularity in several cellular compartments, resulting in similar morphological profiles among the samples. Correlation and clustering analysis showed genotoxic samples grouped separately from non-genotoxic ones. In addition, correlations of the morphological profiles from all samples with existing profiles from a drug repurposing library suggested that the chemical mixture exerts genotoxicity indirectly.

Conclusion

Together, the findings support the contribution of indirect mechanisms to the observed genotoxicity. However, direct genotoxicity cannot be excluded, as mixtures may also contain direct-acting compounds.

1. Introduction

Water sources used for drinking water production are rarely free from chemical contamination. These sources contain complex chemical mixtures of anthropogenic and naturally occurring pollutants which may pose a risk to human health [1]. Such risk increases considering that the average daily water consumption for adults is around 2 to 2.5 L [2] which represents lifelong exposure. Moreover, we consume water from the same water source for long periods of time. Lake Mälaren is the third biggest lake in Sweden serving as one of the most important water sources for drinking water production, supplying drinking water to approximately 20% of the population [3]. However, lake Mälaren is subject to pollution from different contaminants such as pharmaceuticals, personal care products and industrial chemicals due to effluents from wastewater treatment plants and landfill sites [4]. Mälaren is a lake where water overturns occur during spring and autumn seasons resulting in blooms of natural algal cyanotoxins and microcystins [5].

Previous studies using effect-based assessment, have detected genotoxicity in the raw water from lake Mälaren [6, 7]. The studies have indicated a seasonal variation of this bioactivity, with the maximum display during the autumn-winter seasons. The causative compounds for the observed genotoxic effects are still unidentified. Moreover, the studies have also shown that the genotoxic activity was preserved throughout the drinking water treatment process at Görväln drinking water treatment plant (DWTP), which uses lake Mälaren water as its source. In some cases, genotoxicity was also present in finished drinking water but on other occasions it was removed by treatment. Moreover, in the study by Lundqvist *et al* (2024) [7], genotoxic and oxidative stress activities were positively correlated. This could indicate that compounds causing both effects, or compounds with different mode of action (MoA) are co-occurring. Such findings highlight the challenges and limitations faced by conventional drinking water treatment processes, including coagulation, sedimentation, sand filtration, and disinfection, as this treatment process is not designed to fully remove micropollutants [8].

Genotoxicity is a critical safety endpoint in water quality assessment, as genotoxic chemicals can directly or indirectly damage genetic material leading to DNA lesions, mutations and ultimately carcinogenesis [9]. Indirect genotoxicity involves mechanisms that do not physically interact with DNA targets. Instead, DNA damage occurs from secondary mechanisms such as oxidative stress or inhibition of chromatin structures. For indirect genotoxicity, it is generally accepted that safe exposure levels can be derived [10]. Direct genotoxicity refers to physical interactions with DNA structures resulting in adduct formation or strand breaks [11]. As a result, chemicals exerting direct genotoxicity have no concentration threshold, implying that these compounds are regulatory considered to have no safe dose and be potentially carcinogenic [9].

Another challenge in water quality assessment is that it currently relies solely on targeted chemical analysis to evaluate source and finished drinking water. However, this approach only detects known chemicals and fails to account for mixtures, transformation products, or compounds that are toxic at concentrations below the chemical detection limit [12]. For this reason, the use of effect-based methods (EBMs) as a complimentary monitoring tool is

gaining regulatory acceptance in the European Union, as these cell-based assays capture the total toxicity in a sample exerted by both known and unknown chemicals as well as chemical mixtures [13]. In the case of genotoxicity assessment, the micronucleus (MN) assay is one of the most commonly used and recommended *in vitro* tests by regulatory agencies [14]. In addition, assessment of the Nrf2 antioxidant defense pathway activation is another endpoint commonly tested along MN assay, as this bioactivity indicates the presence of compounds inducing oxidative stress [8]. However, the MN assay does not distinguish between direct and indirect genotoxicity. While the Nrf2 assay may indicate indirect genotoxicity, it does not allow for a definitive conclusion about whether the observed effects are direct or indirect.

Cell Painting is a method where exposed cells are stained with several dyes that label multiple organelles in the cell [15, 16]. The cells are then imaged across multiple fluorescent channels; images are analyzed by segmenting individual cells and measuring changes in their morphology. By quantifying such changes as morphological profiles, Cell Painting has been used to group chemical compounds and predict mechanisms and MoA in drug discovery [17] and for toxicological screening to assess chemical safety [18].

The aim of this study was to gain a deeper understanding of the molecular and cellular mechanisms of the genotoxic effects caused by chemical mixtures previously observed in raw and treated drinking water from lake Mälaren [6, 7]. By correlating the morphological changes of cells exposed to either genotoxic or non-genotoxic water samples, as well as comparing with the phenotypic profiles of cell exposed to known genotoxic compounds, this study adds valuable knowledge that could help indicate if the genotoxic effects observed in the water may be caused by direct and/or indirect MoAs.

2. Methods

2.1 Lake Mälaren and Görväln DWTP water sample collection and extraction

Water from lake Mälaren serves as the primary source for Görväln DWTP to produce drinking water for around 700,000 consumers in Stockholm. The abstraction point is located in the deeper part of the lake, beneath the thermocline. This helps protect the raw water supplied to the Görväln DWTP, keeping it cooler and reducing exposure to the summer algal blooms that primarily develop above the thermocline. The full-scale treatment at Görväln DWTP involves low-pressure mechanical filtration, coagulation with aluminum sulfate, sedimentation, rapid sand filtration, biologically activated carbon filtration, primary disinfection with UV light and secondary disinfection step with monochloramine. This DWTP has been operational for around 100 years and was originally designed to remove common raw water macropollutants, such as algae and suspended particles [7]. Consequently, over the past decade, several treatment technologies have been evaluated at pilot scale, including granular activated carbon (GAC) filtration which aims at removing micropollutants and other potentially hazardous chemicals.

Genotoxic activity has been detected in raw water and finished drinking water with the highest peak of activity occurring during late autumn [6, 7]. Considering the aforementioned and the aim of the present study, the sampling strategy was designed to collect water samples during the months with expected increased genotoxic activity in the water, which were carried out during October and November of 2024. Moreover, sampling locations were selected based on the findings from the previous studies. The locations selected included raw water after low-pressure mechanical filtration, water after rapid sand filtration, finished drinking water and water after GAC filtration pilot treatment process. The pilot GAC filter was fed with water from rapid sand filtration. The samples were extracted using solid-phase extraction (SPE) and were tested at relative enrichment factors (REFs) of 6.25–50, with REF 50 representing the highest sample concentration tested. A detailed description is provided in section 1.1 in the Supplementary Material (SM).

2.2 Bioassays for oxidative stress and micronucleus formation

Samples were assessed with strategically selected EBMs relevant to the background and aim of the study. The selected bioassays are responsive to chemical mixtures with similar MoAs and are of relevance to human health. Oxidative stress is an endpoint activated by a wide range of chemicals that is indicative of the presence of reactive oxygen species (ROS) and subsequent activation of the Nrf2 antioxidant pathway. Such an endpoint serves as an environmental sensor to detect chemical hazards in the water environment. Genotoxicity is an endpoint that indicates potential DNA damage, which could eventually result in mutations and other adverse health effects (not directly measured by the MN assay). A detailed description of the bioassays used in this study is provided in **Table 1**.

Oxidative stress was assessed using a reporter-gene assay where the bioactivity cut-off was set at ≥1.5-fold induction. For this endpoint a blank control, denominated Milli-Q water (MQ) SPE control, was included to rule out potential contamination from the SPE columns during extraction. MN formation was evaluated by flow cytometry, and samples were classified as genotoxic or non-genotoxic based on a ≥3.0-fold induction. The final concentration of vehicle controls and reference compounds was set at 1%. Nrf2 bioactivity and genotoxicity responses were normalized to vehicle controls and expressed as fold change. The bioanalytical equivalent concentrations (BEQs) were derived for samples that were bioactive for oxidative stress. Cytotoxicity for both endpoints was also performed to guarantee that the bioassays are conducted under non-cytotoxic conditions. Samples that were below the cytotoxicity thresholds for each endpoint were excluded for further analysis (**Table 1**). Additional information on cell culture maintenance, bioactivity testing and data analysis is presented in sections 1.2 and 1.3 and tBHQ concentration-response curve is shown in **Fig. S1** in the SM.

Table 1. Effect-based methods used, reference compounds, effect concentration levels, induction fold-change to define bioactivity and cytotoxicity threshold.

2.3 Cell Painting assay

2.3.1 Cell exposure and staining

Toxicological endpoint	Cell line	Reference compound	%-effect level chosen to calculate BEQ	Fold-change to define bioactivity	Cytotoxicity test applied and threshold	International Guideline Document [2]
Oxidative stress (Nrf2 activity)	MCF-7 AREc32	*tert*-butylhydroquinone (tBHQ) 0.78 – 25 µM	$EC_{IR1.5}$	≥ 1.5-fold change	MTS/≤80% of vehicle control	-
Genotoxicity (*in vitro* MN formation)	TK6	Mitomycin C 100 – 350 µM	Not applicable [1]	≥ 3.0-fold change	EMA+/≤ 4.0-fold change of vehicle control	OECD 487 [24]

For Cell Painting experiments, U2-OS, CHO-K1 and MCF-7 were used to analyze morphological changes induced by the samples. U2-OS and MCF-7 were selected as these are adherent cells with well-defined morphology that generate rich, high-dimensional profiles suitable for phenotypic profiling [19]. CHO-K1 was selected because this adherent cell line is recommended in the protocol *In vitro* MicroFlow (Litron Laboratories, NY, USA) to assess MN. The TK6 cells used in the MN assay were not used for Cell Painting assays as using suspension cells is methodologically more complex compared to adherent cells. Water samples were analyzed using REFs 50 and 25 and were run in parallel with reference compounds and controls. Mitomycin C (MC, 350 nM) was selected as the reference compound based on its application on the MN assay. Additional phenotypic reference compounds (berberine chloride, etoposide, fenbendazole, hydroxyurea and nocodazole) were initially included based on their ability to induce distinct morphological changes in Cell Painting assays [20, 21]. However, cytochalasin B (CB, 5 µM) (CAS 14930-96-2, purity ≥ 98%, Sigma Aldrich) was the only compound which resembled more closely the morphological changes in the water samples and was selected as phenotypic reference compound for further analysis. The final ethanol concentration of vehicles and samples was set to 1%. The final DMSO concentration of CB was set at 0.5% and for MC at 0.1%. Cell Painting experiments were conducted following the well-established Cell Painting assay protocol [15, 16] with minor modifications. Following exposure cells were stained with a multiplexed fluorescent dye panel targeting the mitochondria, nucleus, cytoplasmic RNA/nucleoli, endoplasmic reticulum, Golgi apparatus/plasma membrane and F-actin cytoskeleton. Details on cell culture maintenance and Cell Painting procedures are shown in sections 1.2 and 1.4 in the SM.

2.3.2 Morphological profiling and analysis

High-throughput fluorescence imaging was performed using nine fields per well across five channels, followed by image quality control, segmentation, and feature extraction using CellProfiler (v 4.3.4). Approximately 1,500 morphological features per cell were quantified across cellular compartments, summarized per image, and normalized to vehicle controls prior to downstream analysis. A detailed description on image acquisition and processing is presented in section 1.5 in the SM.

Phenotypic perturbations were assessed using grit scores and cell counts normalized to the vehicle controls and compared to the negative controls using one-way ANOVA followed by Dunnett's multiple comparison test, with a significance set at $p \leq 0.05$. The top 50 morphological features were selected to characterize treatment-specific profiles using heatmaps, radar plots and multidimensional scaling (MDS), while correlation analysis were performed to compare water samples and reference compounds. An additional correlation analysis using the SPECS drug repurposing set library (https://compoundcenter.scilifelab.se/info/libraries_available_ai) based on U2-OS cells was performed to identify possible genotoxic MoAs. Data analysis and visualization was performed using GraphPad (v 11.0.0), Python 3 and Orange Data Mining (v 3.39.0).

[1] For genotoxicity, no BEQ is calculated. The samples are instead labelled as genotoxic or non-genotoxic based on the ≥ 3.0-fold induction compared to the vehicle control

[2] Referenced *in vitro* assays were performed according to international guideline documents but with minor modifications. A detailed description of the experimental procedures is given in the SM.

3. Results and Discussion

3.1 Cell viability confirms non-cytotoxic exposure conditions

Cell viability assessment in the MN assay showed that none of the water samples were cytotoxic. Although raw water at REF 50 in October displayed a more pronounced reduction in cell viability it was still determined that this sample was non-cytotoxic (SM, **Fig. S2 a – d**). Cell viability assessment in the oxidative stress assay showed that none of the aforementioned samples were cytotoxic (SM, **Fig. S2 e – h**). As a result, all samples were included for further analysis.

3.2 Genotoxicity and oxidative stress persist across the treatment process

In this study, raw, after sand filtration, and drinking water samples during October and November induced MN formation (**Fig. 1 b – d**). Drinking water from October and water after sand filtration from November samples at REF 50 displayed the highest genotoxic activity (**Table 2**). Such findings may be indicative of the presence of compounds inducing genotoxicity that the conventional treatment process is not able to fully remove. Conversely, none of the GAC filtration samples were genotoxic (**Fig. 1 a**), suggesting that this pilot treatment process is more efficient at removing the genotoxic compounds. With regard to the activation of the Nrf2 pathway, all water samples were bioactive (**Fig. 1 e - h**). However, GAC filtration samples displayed the lowest bioactivity although both values remained above the detection limit (10.5 µg tBHQeq/L). In contrast, the genotoxic samples exhibited bioactivities above the cut-off limit, with the drinking water sample in October showing the highest response. The calculated BEQs ranged from 37.5 to 112.3 µg tBHQeq/L, with water after

sand filtration sample in November exhibiting the highest potency (**Table 2**). The findings on Nrf2 bioactivity indicate the presence of oxidative stress across the full-scale treatment process and further corroborate the removal efficiency of GAC filtration.

Genotoxicity [22-24] and oxidative stress [25–27] have been reported from source water through conventional treatment and into finished drinking water, although treatment efficiency varies among systems. At the Görväln DWTP, both bioactivities have previously shown seasonal variation, with the highest activity during autumn [6, 7]. The responses observed in the present study were broadly consistent with previous measurements at the DWTP. Genotoxic and oxidative stress were first reported during November and May of 2019 [6], where genotoxicity was only detected in water after sand filtration and oxidative stress was detected in raw and after sand filtration waters (70 and 143 µg tBHQeq/L), at levels which were similar to those obtained in this study (61 and 112 µg tBHQeq/L). A more recent study [7] with samples from October and November 2021, showed that raw water displayed higher genotoxicity. However, water after sand filtration and drinking water displayed lower genotoxicity. The Nrf2 bioactivities for raw water in October (3 µg tBHQeq/L), water after sand filtration (27 and 48 µg tBHQeq/L) and drinking water (23 and 43 µg tBHQeq/L) were lower than our findings. Only bioactivity for raw water in November (77 µg tBHQeq/L) was higher than our findings. Together, these findings support the recurrent occurrence of genotoxic and oxidative stress bioactivity throughout the conventional treatment process during autumn. GAC filtration can effectively remove complex chemical mixtures, including micropollutants, transformation products, and natural toxins [28], consistent with its previously demonstrated removal of genotoxic and oxidative-stress bioactivity at the Görväln DWTP [6, 7]

Table 2. Fold change induction for genotoxicity and oxidative stress bioactivities for all collected samples and BEQ values of Nrf2 bioactive samples. Data is presented as mean ± SD, n= 4 for MN (one independent experiment with four technical replicates per concentration), n= 8 for Nf2 (two independent experiments with four technical replicates per concentration).

			MN fold change (≥ 3.0-fold)		Nrf2 fold change (≥ 1.5-fold)		Nrf2 bioactivity
	Sample	**Month**	**REF 25**	**REF 50**	**REF 25**	**REF 50**	**BEQ (µg tBHQeq/L)**
Pilot treatment process	**GAC filtration**	October	-	-	-	2.1	18.6 ± 7.6
		November	-	-	-	2.0	15.2 ± 1.5
Conventional treatment process	**Raw water**	October	5.0	9.0	1.7	3.9	37.5 ± 8.5
		November	-	3.0	3.9	8.4	60.8 ± 15.8
	Sand filtration	October	3.0	8.0	5.6	11.3	104.2 ± 46.6
		November	3.0	14.0	5.9	11.4	112.3 ± 56.6
	Drinking water	October	4.0	24.0	6.2	13.8	95.1 ± 20.7
		November	-	8.0	4.6	11.3	79.5 ± 3.2

3.3 Water samples induce concentration-dependent morphological perturbation and cell loss

The findings on morphological perturbation showed that all samples significantly induced changes on the cells compared to the negative controls following a concentration-dependent pattern in all cell lines. CB and MC were also significantly different from the solvent control in U2-OS and CHO-K1 cells, whereas only CB was significantly different from the control in MCF-7 (**Fig. 2 a - c**). Interestingly, MC had the highest perturbation in CHO-K1 cells, which is a cell line commonly used for *in vitro* MN assessment and known for its sensitivity to screen chromosomal damage [29]. Overall, U2-OS displayed the highest level of morphological perturbation for all samples in contrast with CHO-K1 and MCF-7. Detailed grit scores are given in **Table S1** in the SM. Changes in cell count showed that all genotoxic water samples at REF 50 induced a significant decrease in cell count compared with the negative controls, in a concentration-dependent manner. Among the reference compounds, CB significantly reduced cell count in all three cell lines, whereas MC only induced a significant decrease in CHO-K1 cells. Overall, samples induced a comparable reduction in cell count across the three cell lines (**Fig. 2 d – f**). Detailed cell count data are provided in **Table S2** in the SM. Cell Painting images of GAC filtration (non-genotoxic) and drinking water (genotoxic) samples collected in October at REFs 25 and 50 further illustrate the morphological alterations and reduced cell count. The drinking water sample showed reduced staining intensity, altered staining distribution, and lower cell density across all cell lines compared with GAC filtration (**Fig. 2g – i**), consistent with the measured morphological perturbation and cell count. Cell Painting images for all the samples and cell lines are shown in **Figs. S3 - S5** in the SM.

These findings highlight the ability of morphological profiling to capture phenotypic responses induced by complex environmental mixtures in water samples. Moreover, the varying response magnitudes observed across cell lines further highlight the sensitivity of different cell lines to chemical mixtures. In addition, the observed phenotypic alterations may be associated with sub-cytotoxic effects such as reduced cellular proliferation or early stress responses rather than direct cytotoxicity [15, 30]. The results herein align with a study where the observed phenotypic responses and cell count of different cell lines including U2-OS and MCF-7, support morphological profiling as a sensitive approach for capturing biological effects induced by chemical mixtures in a concentration-dependent pattern [31].

3.4 Genotoxic samples share a common morphological profile centered on the nucleus, mitochondria, and nucleoli

Heatmaps and radar plots were generated to compare the phenotypic profiles of the water samples and reference compounds. In this instance, genotoxic samples and CB exhibited similar morphological alterations across cell lines, distinct from the negative controls. Genotoxic water samples showed concentration-dependent decreases in nuclear area and shape features, including area, length, diameter, convex area, perimeter, and radius, together with increased granularity across multiple cellular compartments such as the nucleus, cytoplasm, whole cell as well as reduced mitochondrial integrated intensity.

Cell line-specific alterations included increased RNA/nucleoli granularity in U2-OS and endoplasmic reticulum-related changes in CHO-K1, while MC increased nuclear area features in U2-OS and CHO-K1 but not in MCF-7 (**Fig. 3 a**–**c**; **Figs. S6**–**S8**). Radar plots confirmed similar phenotypic profiles among genotoxic samples across cell lines, with minor sample and cell specific variations (**Figs. S9**–**S11**). Changes in nuclear, mitochondrial, and nucleoli features indicated that these compartments were major targets for the chemical mixture, with representative profile similarities shown in **Fig. 3 d – e**. These alterations suggest changes in intracellular organization, including reduced nuclear proximity to surrounding cellular structures consistent with profiling studies showing that morphological features capture changes in cell reorganization [19, 30].

The decrease in nuclear area features across all cell lines indicates reduced nuclear size, consistent with the sensitivity of nuclear morphology to chemical-induced perturbations [15, 20]. Such changes may reflect nuclear condensation which has been associated with cellular stress and genotoxic responses [32]. Decreased correlations between mitochondrial and cytoskeletal or nuclear features further indicate altered subcellular organization and mitochondrial activity. Increased granularity across multiple compartments may also reflect changes in intracellular organization and structural condensation [15, 33-35]. Finally, increased correlations between the nucleus and nucleoli may indicate altered structural coordination between these compartments, consistent with the nucleolus being dynamically integrated into nuclear organization and influencing nuclear architecture [36].

3.5 Genotoxic and non-genotoxic samples form distinct phenotypic clusters

Multivariate analysis was performed to compare phenotypic similarities among water samples and assess whether a common genotoxic profile persisted across the conventional treatment process and was removed by GAC filtration. MDS showed distinct clustering of REF 50 and REF 25 across all cell lines, consistent with concentration-dependent morphological responses **(Fig. 4)**. Genotoxic samples also clustered separately from non-genotoxic samples in U2-OS and MCF-7 cells (Kruskal stress= 0.63; 0.60, **Fig. 4a** & **e**), whereas this separation was less evident in CHO-K1 (Kruskal stress = 0.11, F**ig. 4c**). CB showed similarity to genotoxic samples the phenotypic, but the differences were sufficient to prevent them from clustering together. Instead, MC displayed a markedly different profile from all samples and CB. Correlation analysis further showed positive correlations among genotoxic samples across all cell lines. Correlation coefficients and relationship levels are presented in **Table S3.** In U2-OS, genotoxic samples and CB showed moderate to very strong correlations (r= 0.41–0.91), except with GAC samples (**Fig. 4 b**). CHO-K1 showed moderate to very strong correlations (r= 0.33-0.94) among genotoxic samples and CB, but also strong to very strong correlations with non-genotoxic REF 50 samples (r= 0.75-0.89, **Fig. 4 d**). In MCF-7, genotoxic samples and CB showed strong-to-very strong correlations (r = 0.73–0.89), particularly at REF 50, while GAC samples showed moderate correlations (**Fig. 4 f**). Correlations are shown in **Fig. S12**.

The clustering and correlation patterns indicate that genotoxic samples shared a common morphological profile across the conventional treatment process, whereas GAC filtration samples showed distinct profiles, further confirming removal efficiency of the bioactivity associated with genotoxicity. Differences among cell lines further indicate cell-specific responses and sensitivity. U2-OS provided the clearest separation between genotoxic and non-genotoxic samples, consistent with their established use in Cell Painting because of its well-defined morphology, rich organelle structure, and ability to generate distinct phenotypic responses to cellular perturbations [37]. MCF-7 showed a similar pattern, although stronger correlations were more apparent at REF 50, suggesting a higher threshold for detectable morphological perturbation. MCF-7 cells are used in morphology profiling to assess phenotypic responses induced by chemical perturbations, thus supporting their utility in assessing compound-induced cellular effects [20, 31]. In contrast, CHO-K1 showed less distinct separation and more uniform correlations across samples, despite its established sensitivity for detecting chromosomal damage [29]. This may reflect their more limited use for Cell Painting compared with cell lines such as U2-OS, Caco-2, and A549 [30, 31].

3.6 Correlation with reference compounds points to an indirect genotoxic mechanism

To investigate potential mechanisms underlying the genotoxicity, morphological profiles of the water samples and reference compounds were compared with 5270 compounds from the SPECS drug repurposing library using correlation analysis. U2-OS profiles were used because the SPECS reference profiles were generated in this cell line with no available for CHO-K1 and MCF-7. Of the 5270 compounds, 50 showed positive correlations (r = 0.35–0.66) with at least two samples, including GAC filtration and CB (**Table 3**). These compounds represented 11 mechanistic categories and 28 specific MoAs. Thirty-seven compounds correlated with at least two samples and CB, whereas 13 correlated exclusively with GAC samples. A total of 20 compounds had MoAs potentially relevant to genotoxicity and were mainly associated with membrane perturbation and epigenetic modulation mechanistic categories (Table 3). Membrane perturbation can induce oxidative stress through disruption of membrane integrity, leading to increased ROS production and subsequent indirect DNA damage [38, 39]. In this category, four compounds showed moderate to strong correlations with all genotoxic samples and CB (**Table 3**). Conversely, epigenetic modulation may alter gene expression patterns involved in DNA repair and cell cycle regulation [40, 41] which includes silent information regulator transcript (SIRT) inhibition, kinase inhibition/histone deacetylase (HDAC) inhibition, HDAC inhibition and bromodomain inhibition MoAs. One SIRT inhibitor showed moderate correlations with most genotoxic samples and CB, one kinase/HDAC inhibitor showed moderate to strong correlations with all genotoxic samples and CB, four HDAC inhibitors correlated moderately to strongly with genotoxic and weakly to moderately with non-genotoxic samples but not CB, and ten bromodomain inhibitors showed moderate to strong correlations with genotoxic samples and CB (**Table 3**). The remaining 17 compounds represented eight mechanistic categories, including neurotransmitter receptor and endocrine pathway modulation, and were not considered relevant to potential genotoxic mechanisms (**Table S4**). The 13 compounds correlated exclusively with GAC samples showed mostly weak correlations across MoAs including HDAC inhibition and AMPK activation (**Table S5**). In contrast, 31 compounds showed strong correlations exclusively with MC but not with water samples or CB. Of these, 24 were associated with DNA interaction/disruption, DNA replication/transcription, DNA repair, or cell-cycle regulation (Table S6). Such correlations potentially indicate that MC exerts its MoA through direct DNA damage by acting as an alkylating agent, inhibiting DNA synthesis and leading to cell death [42].

The combined evidence from MN formation, oxidative stress, morphological profiling, sample clustering, SPECS correlations and lack of correlations with compounds associated with MC provides evidence that indirect mechanisms contribute substantially to the observed genotoxicity. The morphological similarities among genotoxic samples and their correlations with compounds associated with membrane perturbation and epigenetic modulation support a

potential mechanism involving cellular stress, mitochondrial dysfunction, and altered regulation of pathways related to DNA repair and cell cycle control [40, 41, 43]. Moreover, this data suggests that the unknown chemical mixture may generate elevated levels of ROS, leading to mitochondrial dysfunction and oxidative stress, which in turn could indirectly affect DNA and RNA structures. The absence of similarity between genotoxic samples and MC, a direct-acting genotoxicant, further supports this interpretation. The positive correlations between genotoxic samples and CB, a non-genotoxic F-actin polymerization inhibitor, may also reflect structural perturbations associated with cellular stress rather than direct DNA damage. However, these findings do not exclude direct genotoxicity, as the observed effects may arise from mixtures containing both direct- and indirect-acting compounds. Similarly, the correlations between MN formation and Nrf2 activity previously observed at the Görväln DWTP [7] support a role for oxidative stress but cannot distinguish between a purely indirect mechanism and co-occurring direct and indirect genotoxicants. Because the compounds responsible for the observed activity remain unidentified, it is not possible to determine if this effect has a safe exposure level or not.

Table 3. Correlations between water samples and SPECS drug repurposing set in U2-OS cells with indications of possible genotoxic MoA. The table shows the positive correlation range of water samples and CB with SPECS compounds as well as the mechanistic category and specific MoA in which the correlations were classified. Correlation are indicated with the ● symbol. GAC= GAC filtration, RW= Raw water, SF= Sand filtration and DW= Drinking water.

4. Conclusion

In this study, we applied EBMs and morphological profiling to investigate the mechanisms underlying the genotoxicity previously observed at several stages of the conventional drinking water treatment process at the Görväln DWTP. All samples, except GAC filtration, exhibited genotoxicity and oxidative stress, while all water samples induced significant morphological perturbations. Genotoxic samples showed concentration-dependent decreases in nuclear area features and increases in granularity across multiple cellular compartments, resulting in similar morphological profiles identifying the nucleus, mitochondria, and nucleoli as the main targets. These findings indicate that the unknown genotoxic compounds persist throughout the conventional treatment process. Clustering and correlation analyses further supported the effectiveness of GAC treatment in removing the bioactivity associated with the genotoxic samples. Correlation with SPECS compounds provided additional insight into potential MoAs, with phenotypic similarities to compounds associated with membrane perturbation and epigenetic regulation supporting a substantial contribution of indirect mechanisms to the observed genotoxicity. However, direct-acting genotoxicants cannot be excluded, as the observed effects may result from mixtures containing both direct- and indirect-acting compounds. Overall, integrating EBMs with Cell Painting provided mechanistic information on the biological effects of complex drinking water mixtures while highlighting the challenges of attributing mixture effects to specific MoAs.

Declarations

Acknowledgments

This study was financially supported by the Swedish University of Agricultural Sciences. **J.L.** acknowledges funding from Horizon Europe (grant agreement 101057014, PARC). **O.S.** acknowledges funding from FORMAS (grant 2025-02678), and the Swedish strategic research programme eSSENCE. The authors acknowledge the support from the Chemical Biology Consortium Sweden (CBCS), node UU, a national research infrastructure funded by the Swedish Research Council (dr.nr.2021-00179) and SciLifeLab.

Author contributions

A.C.M. Conceptualization, Data curation, Formal analysis, Investigation, Methodology, Project administration, Validation, Visualization, Writing – original draft, Writing – review and editing. **M.J.** Investigation, Methodology, Project administration, Writing – review and editing. **J.R.** Conceptualization, Data curation, Formal analysis, Investigation, Methodology, Writing – review and editing. **M.L.** Data curation, Formal analysis, Methodology, Software, Visualization, Writing – review and editing. **J.C.P.** Conceptualization, Investigation, Methodology, Supervision, Software, Writing – review and editing. **O.S.** Conceptualization, Investigation, Methodology, Resources, Supervision, Writing – review and editing. **J.L.** Conceptualization, Funding acquisition, Investigation, Methodology, Project administration, Resources, Supervision, Writing – review and editing.

Research data

The data supporting the findings of this study is available in this article and in the Supplementary Material associated with this study. Additional data is available from the corresponding author upon reasonable request.

Declaration of Competing Interest

J.L. is the founder and owner of BioCell Analytica Uppsala AB, a company providing effect-based testing services to the water sector. **A.C.M.** has been employed by the same company. All other authors declare that they have no known competing financial interests or personal relationships that could have appeared to influence the work reported in this paper.

References

1. M.L. De Baat, R. Van der Oost, G.H. Van der Lee, N. Wieringa, T. Hamers, P.F.M. Verdonschot, P. De Voogt, M.H.S. Kraak, Advancements in effect-based surface water quality assessment, Water Research 183 (2020). https://doi.org/10.1016/j.watres.2020.116017.

Compound	Mechanistic category	Specific MoA	Correlation range with water samples	GAC Oct	GAC Nov	RW Oct	RW Nov	SF Oct	SF Nov	DW Oct	DW Nov	Cl
Benzyldimethylhexadecylammonium chloride hydrate	Membrane perturbation	Membrane disruption/integrity/ inhibition	0.55 – 0.65 Moderate - Strong			●	●	●	●	●	●	●
Chlorhexidine dihydrochloride hydrate			0.53 – 0.64 Moderate - Strong			●	●	●	●	●	●	●
Methylbenzethonium chloride			0.45 – 0.56 Moderate			●	●	●	●		●	●
Domiphen bromide			0.49 – 0.58 Moderate - Strong			●				●		●
Tenovin-6	Epigenetic modulation	SIRT inhibition	0.49 – 0.57 Moderate				●	●	●	●		●
CUDC-101		Kinase inhibition (EGFR & ERBB2) & HDAC inhibition	0.50 – 0.61 Moderate - Strong			●	●	●	●	●	●	●
CI994 (Tacedinaline)		HDAC inhibition	0.51 – 0.63 Moderate - Strong			●	●	●	●	●	●	
RG2833 (RGFP109)			0.35 – 0.59 Weak - Moderate	●		●	●	●	●	●	●	
SBHA			0.35 – 0.55 Weak - Moderate	●	●	●	●	●	●	●		
Nexturastat A			0.41 – 0.53 Weak - Moderate	●	●	●	●	●			●	
(+)-JQ1		Bromodomain inhibition	0.55 – 0.66 Moderate - Strong				●	●	●	●	●	●
ARV-825			0.55 – 0.66 Moderate - Strong				●	●	●	●	●	●
BET-BAY 002			0.54 – 0.64 Moderate - Strong				●	●	●	●	●	●
Bromosporine			0.50 – 0.64 Moderate - Strong				●	●	●	●	●	●
CPI-203			0.54 – 0.61				●	●	●	●	●	●

		Moderate - Strong						
CPI-0610		0.57 – 0.66 Moderate - Strong	•		•	•	•	•
OTX015		0.52 – 0.60 Moderate - Strong	•	•	•	•	•	•
I-BET151 (GSK1210151A)		0.53 – 0.59 Moderate	•	•	•	•	•	
I-BET-762		0.55 – 0.59 Moderate	•	•	•	•	•	
PFI-1(PF-6405761)		0.51 – 0.56 Moderate	•	•	•	•	•	

2. EFSA Panel on Dietetic Products Nutrition, and Allergies (NDA), Scientific opinion on dietary reference values for water, EFSA J. 8 (2010) 1459. https://doi.org/10.2903/j.efsa.2010.1459
3. L. Sonesten, K. Wallman, T. Axenrot, U. Beier, S. Drakare, F. Ecke, et al., Lake Mälaren: Development of Environmental Conditions 1965–2011 (Mälaren Tillståndsutvecklingen 1965–2011), Swedish University of Agricultural Sciences, Department of Aquatic Sciences and Assessment, (2013).
4. A.-L. Rehrl, O. Golovko, L. Ahrens, S. Köhler, Spatial and seasonal trends of organic micropollutants in Sweden's most important drinking water reservoir, Chemosphere 249 (2020) 126168. https://doi.org/https://doi.org/10.1016/j.chemosphere.2020.126168.
5. E. Willén, Phytoplankton and Water Quality Characterization: Experiences from the Swedish Large Lakes Mälaren, Hjälmaren, Vättern and Vänern, AMBIO: A Journal of the Human Environment 30(8) (2001) 529–537, 9.
6. M. Yu, E. Lavonen, A. Oskarsson, J. Lundqvist, Removal of oxidative stress and genotoxic activities during drinking water production by ozonation and granular activated carbon filtration, Environmental Sciences Europe 33(1) (2021) 124. https://doi.org/10.1186/s12302-021-00567-y.
7. J. Lundqvist, E. Lavonen, G. Mandava, E. Selin, H. Ejhed, A. Oskarsson, Effect-based monitoring of chemical hazards in drinking water from source to tap: seasonal trends over 2 years of sampling, Environmental Sciences Europe 36(1) (2024). https://doi.org/10.1186/s12302-024-00875-z.
8. A. Oskarsson, A.K. Rosenmai, G. Mandava, A. Johannisson, A. Holmes, R. Tröger, J. Lundqvist, Assessment of source and treated water quality in seven drinking water treatment plants by in vitro bioassays - Oxidative stress and antiandrogenic effects after artificial infiltration, Science of the Total Environment 758 (2021). https://doi.org/10.1016/j.scitotenv.2020.144001.
9. World Health Organization. Guidelines for drinking-water quality: fourth edition incorporating the first and second addenda, World Health Organization, (2022). https://www.who.int/publications/i/item/9789240045064
10. M. Kirsch-Volders, M. Aardema, A. Elhajouji, Concepts of threshold in mutagenesis and carcinogenesis, Mutation Research/Genetic Toxicology and Environmental Mutagenesis 464(1) (2000) 3–11. https://doi.org/https://doi.org/10.1016/S1383-5718(99)00161-8.
11. World Health Organization, Food and Agriculture Organization. Principles and methods for the risk assessment of chemicals: Chapter 4.5 – Genotoxicity, WHO Environmental Health Criteria, (2019). https://www.who.int/docs/default-source/food-safety/ehc-240-chapter-4-5-genotoxicity-draft-dec-2019.pdf
12. P.A. Neale, B.I. Escher, M.L. de Baat, M. Dechesne, M.M.L. Dingemans, J. Enault, G.J. Pronk, P.W.M.H. Smeets, F.D.L. Leusch, Application of Effect-Based Methods to Water Quality Monitoring: Answering Frequently Asked Questions by Water Quality Managers, Regulators, and Policy Makers, Environmental Science & Technology 57(15) (2023) 6023–6032. https://doi.org/10.1021/acs.est.2c06365.
13. W. Brack, S.A. Aissa, T. Backhaus, V. Dulio, B.I. Escher, M. Faust, K. Hilscherova, J. Hollender, H. Hollert, C. Müller, J. Munthe, L. Posthuma, T.-B. Seiler, J. Slobodnik, I. Teodorovic, A.J. Tindall, G. de Aragão Umbuzeiro, X. Zhang, R. Altenburger, Effect-based methods are key. The European Collaborative Project SOLUTIONS recommends integrating effect-based methods for diagnosis and monitoring of water quality, Environmental Sciences Europe 31(1) (2019) 10. https://doi.org/10.1186/s12302-019-0192-2.
14. D. Kirkland, P. Kasper, H.-J. Martus, L. Müller, J. van Benthem, F. Madia, R. Corvi, Updated recommended lists of genotoxic and non-genotoxic chemicals for assessment of the performance of new or improved genotoxicity tests, Mutation Research/Genetic Toxicology and Environmental Mutagenesis 795 (2016) 7–30. https://doi.org/https://doi.org/10.1016/j.mrgentox.2015.10.006.
15. M.A. Bray, S. Singh, H. Han, C.T. Davis, B. Borgeson, C. Hartland, M. Kost-Alimova, S.M. Gustafsdottir, C.C. Gibson, A.E. Carpenter, Cell Painting, a high-content image-based assay for morphological profiling using multiplexed fluorescent dyes, Nat Protoc 11(9) (2016) 1757–74. https://doi.org/10.1038/nprot.2016.105.
16. S. Seal, M.A. Trapotsi, O. Spjuth, S. Singh, J. Carreras-Puigvert, N. Greene, A. Bender, A.E. Carpenter, Cell Painting: a decade of discovery and innovation in cellular imaging, Nat Methods 22(2) (2025) 254–268. https://doi.org/10.1038/s41592-024-02528-8.

17. J.D. Ewald, K.L. Titterton, A. Bäuerle, A. Beatson, D.A. Boiko, A. Cabrera Á, J. Cheah, B.A. Cimini, B. Gorissen, T. Jones, K.J. Karczewski, D. Rouquie, S. Seal, E. Weisbart, B. White, A.E. Carpenter, S. Singh, Cell Painting for cytotoxicity and mode-of-action analysis in primary human hepatocytes, bioRxiv (2025). https://doi.org/10.1101/2025.01.22.634152.
18. J. Nyffeler, C. Willis, F.R. Harris, M.J. Foster, B. Chambers, M. Culbreth, R.E. Brockway, S. Davidson-Fritz, D. Dawson, I. Shah, K.P. Friedman, D. Chang, L.J. Everett, J.F. Wambaugh, G. Patlewicz, J.A. Harrill, Application of Cell Painting for chemical hazard evaluation in support of screening-level chemical assessments, Toxicol Appl Pharmacol 468 (2023) 116513. https://doi.org/10.1016/j.taap.2023.116513.
19. J.C. Caicedo, S. Singh, A.E. Carpenter, Applications in image-based profiling of perturbations, Curr Opin Biotechnol 39 (2016) 134–142. https://doi.org/10.1016/j.copbio.2016.04.003.
20. C. Willis, J. Nyffeler, J. Harrill, Phenotypic Profiling of Reference Chemicals across Biologically Diverse Cell Types Using the Cell Painting Assay, SLAS Discov 25(7) (2020) 755–769. https://doi.org/10.1177/2472555220928004.
21. M. Akbarzadeh, I. Deipenwisch, B. Schoelermann, A. Pahl, S. Sievers, S. Ziegler, H. Waldmann, Morphological profiling by means of the Cell Painting assay enables identification of tubulin-targeting compounds, Cell Chem Biol 29(6) (2022) 1053–1064.e3. https://doi.org/10.1016/j.chembiol.2021.12.009.
22. D. Wang, Z. Xu, Y. Zhao, X. Yan, J. Shi, Change of genotoxicity for raw and finished water: role of purification processes, Chemosphere 83(1) (2011) 14–20. https://doi.org/10.1016/j.chemosphere.2011.01.039.
23. P. Shi, S. Zhou, H. Xiao, J. Qiu, A. Li, Q. Zhou, Y. Pan, H. Hollert, Toxicological and chemical insights into representative source and drinking water in eastern China, Environmental pollution 233 (2018) 35–44.
24. D. Feretti, M. Acito, M. Dettori, E. Ceretti, C. Fatigoni, S. Posadino, I. Zerbini, M. Villarini, M. Moretti, P. Castiglia, A. Azara, Genotoxicity of source, treated and distributed water from four drinking water treatment plants supplied by surface water in Sardinia, Italy, Environ Res 185 (2020) 109385. https://doi.org/10.1016/j.envres.2020.109385.
25. B.I. Escher, M. Dutt, E. Maylin, J.Y. Tang, S. Toze, C.R. Wolf, M. Lang, Water quality assessment using the AREc32 reporter gene assay indicative of the oxidative stress response pathway, J Environ Monit 14(11) (2012) 2877–85. https://doi.org/10.1039/c2em30506b.
26. A. Hebert, C. Feliers, C. Lecarpentier, P.A. Neale, R. Schlichting, S. Thibert, B.I. Escher, Bioanalytical assessment of adaptive stress responses in drinking water: A predictive tool to differentiate between micropollutants and disinfection by-products, Water Research 132 (2018) 340–349. https://doi.org/10.1016/j.watres.2017.12.078.
27. P.A. Neale, C. Feliers, L. Glauch, M. König, C. Lecarpentier, R. Schlichting, S. Thibert, B.I. Escher, Application of in vitro bioassays for water quality monitoring in three drinking water treatment plants using different treatment processes including biological treatment, nanofiltration and ozonation coupled with disinfection, Environmental Science: Water Research & Technology 6(9) (2020) 2444–2453. https://doi.org/10.1039/C9EW00987F.
28. A.M. Brunner, C. Bertelkamp, M.M.L. Dingemans, A. Kolkman, B. Wols, D. Harmsen, W. Siegers, B.J. Martijn, W.A. Oorthuizen, T.L. ter Laak, Integration of target analyses, non-target screening and effect-based monitoring to assess OMP related water quality changes in drinking water treatment, Science of the Total Environment 705 (2020). https://doi.org/10.1016/j.scitotenv.2019.135779.
29. Organisation for Economic Co-operation and Development (OECD), Test No. 487: In vitro mammalian cell micronucleus test, OECD Guidelines for the Testing of Chemicals, (2023). https://doi.org/10.1787/9789264264861-en
30. M.H. Rohban, S. Singh, X. Wu, J.B. Berthet, M.A. Bray, Y. Shrestha, X. Varelas, J.S. Boehm, A.E. Carpenter, Systematic morphological profiling of human gene and allele function via Cell Painting, Elife 6 (2017). https://doi.org/10.7554/eLife.24060.
31. J. Rietdijk, T. Aggarwal, P. Georgieva, M. Lapins, J. Carreras-Puigvert, O. Spjuth, Morphological profiling of environmental chemicals enables efficient and untargeted exploration of combination effects, Sci Total Environ 832 (2022) 155058. https://doi.org/10.1016/j.scitotenv.2022.155058.
32. R. Rose, N. Peschke, E. Nigi, M. Gelléri, S. Ritz, C. Cremer, H.J. Luhmann, A. Sinning, Chromatin compaction precedes apoptosis in developing neurons, Commun Biol 5(1) (2022) 797. https://doi.org/10.1038/s42003-022-03704-2.
33. G.P. Way, M. Kost-Alimova, T. Shibue, W.F. Harrington, S. Gill, F. Piccioni, T. Becker, H. Shafqat-Abbasi, W.C. Hahn, A.E. Carpenter, F. Vazquez, S. Singh, Predicting cell health phenotypes using image-based morphology profiling, Mol Biol Cell 32(9) (2021) 995–1005. https://doi.org/10.1091/mbc.E20-12-0784.
34. S. Seal, J. Carreras-Puigvert, S. Singh, A.E. Carpenter, O. Spjuth, A. Bender, From pixels to phenotypes: Integrating image-based profiling with cell health data as BioMorph features improves interpretability, Mol Biol Cell 35(3) (2024) mr2. https://doi.org/10.1091/mbc.E23-08-0298.
35. M. Tegtmeyer, J. Arora, S. Asgari, B.A. Cimini, A. Nadig, E. Peirent, D. Liyanage, G.P. Way, E. Weisbart, A. Nathan, T. Amariuta, K. Eggan, M. Haghighi, S.A. McCarroll, L. O'Connor, A.E. Carpenter, S. Singh, R. Nehme, S. Raychaudhuri, High-dimensional phenotyping to define the genetic basis of cellular morphology, Nat Commun 15(1) (2024) 347. https://doi.org/10.1038/s41467-023-44045-w.
36. C. Wang, H. Ma, S.J. Baserga, T. Pederson, S. Huang, Nucleolar structure connects with global nuclear organization, Mol Biol Cell 34(12) (2023) ar114. https://doi.org/10.1091/mbc.E23-02-0062.
37. M.A. Bray, S.M. Gustafsdottir, M.H. Rohban, S. Singh, V. Ljosa, K.L. Sokolnicki, J.A. Bittker, N.E. Bodycombe, V. Dancík, T.P. Hasaka, C.S. Hon, M.M. Kemp, K. Li, D. Walpita, M.J. Wawer, T.R. Golub, S.L. Schreiber, P.A. Clemons, A.F. Shamji, A.E. Carpenter, A dataset of images and morphological profiles of 30 000 small-molecule treatments using the Cell Painting assay, Gigascience 6(12) (2017) 1–5. https://doi.org/10.1093/gigascience/giw014.
38. M.S. Cooke, M.D. Evans, M. Dizdaroglu, J. Lunec, Oxidative DNA damage: mechanisms, mutation, and disease, Faseb j 17(10) (2003) 1195–214. https://doi.org/10.1096/fj.02-0752rev.
39. M. Valko, C.J. Rhodes, J. Moncol, M. Izakovic, M. Mazur, Free radicals, metals and antioxidants in oxidative stress-induced cancer, Chem Biol Interact 160(1) (2006) 1–40. https://doi.org/10.1016/j.cbi.2005.12.009.

40. M. Christmann, B. Kaina, Epigenetic regulation of DNA repair genes and implications for tumor therapy, Mutat Res Rev Mutat Res 780 (2019) 15–28. https://doi.org/10.1016/j.mrrev.2017.10.001 .
41. A. Fernandez, C. O'Leary, K.J. O'Byrne, J. Burgess, D.J. Richard, A. Suraweera, Epigenetic Mechanisms in DNA Double Strand Break Repair: A Clinical Review, Front Mol Biosci 8 (2021) 685440. https://doi.org/10.3389/fmolb.2021.685440.
42. M.M. Paz, X. Zhang, J. Lu, A. Holmgren, A new mechanism of action for the anticancer drug mitomycin C: mechanism-based inhibition of thioredoxin reductase, Chem Res Toxicol 25(7) (2012) 1502–11. https://doi.org/10.1021/tx3002065.
43. A. Ayala, M.F. Muñoz, S. Argüelles, Lipid peroxidation: production, metabolism, and signaling mechanisms of malondialdehyde and 4-hydroxy-2-nonenal, Oxid Med Cell Longev 2014 (2014) 360438. https://doi.org/10.1155/2014/360438.

Figures

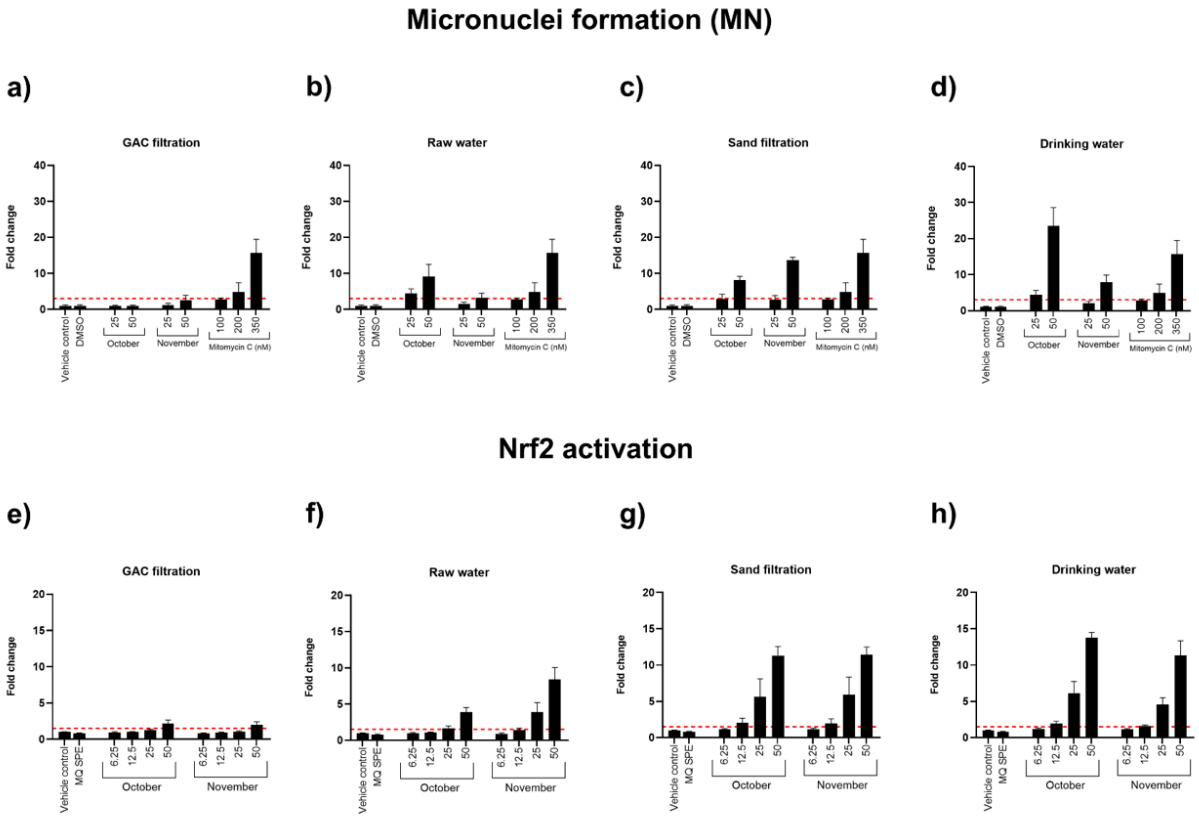


Figure 1

Genotoxicity assessment (MN) and activation of the Nrf2 transcription factor indicative of oxidative stress. In panels **a) - d)**, MN in TK6 cells exposed to water samples and MC (100, 200 and 350 nM) for 24 hrs. The dotted line represents the cut-off limit in fold change (≥ 3.0) for defining genotoxicity. In panels **e) – h)**, Nrf2 bioactivity in MCF-7 AREc32 cells exposed to water samples and MQ SPE for 24 hrs. The dotted line represents the bioactivity cut-off limit in fold change (≥ 1.5) for defining bioactive samples. In both cell lines, samples were categorized as **a)** & **e)** GAC filtration, **b)** & **f)** Raw water, **c)**& **g)** Sand filtration and **d)** & **h)** Drinking water. All samples were assessed in October and November of 2024. Sample concentrations are expressed as REF 25-50 for MN and REF 6.25 – 50 for Nrf2 activity. Data is presented as mean ± SD, n= 4 for MN (one independent experiment with four technical replicates per concentration), n= 8 for Nf2 (two independent experiments with four technical replicates per concentration).

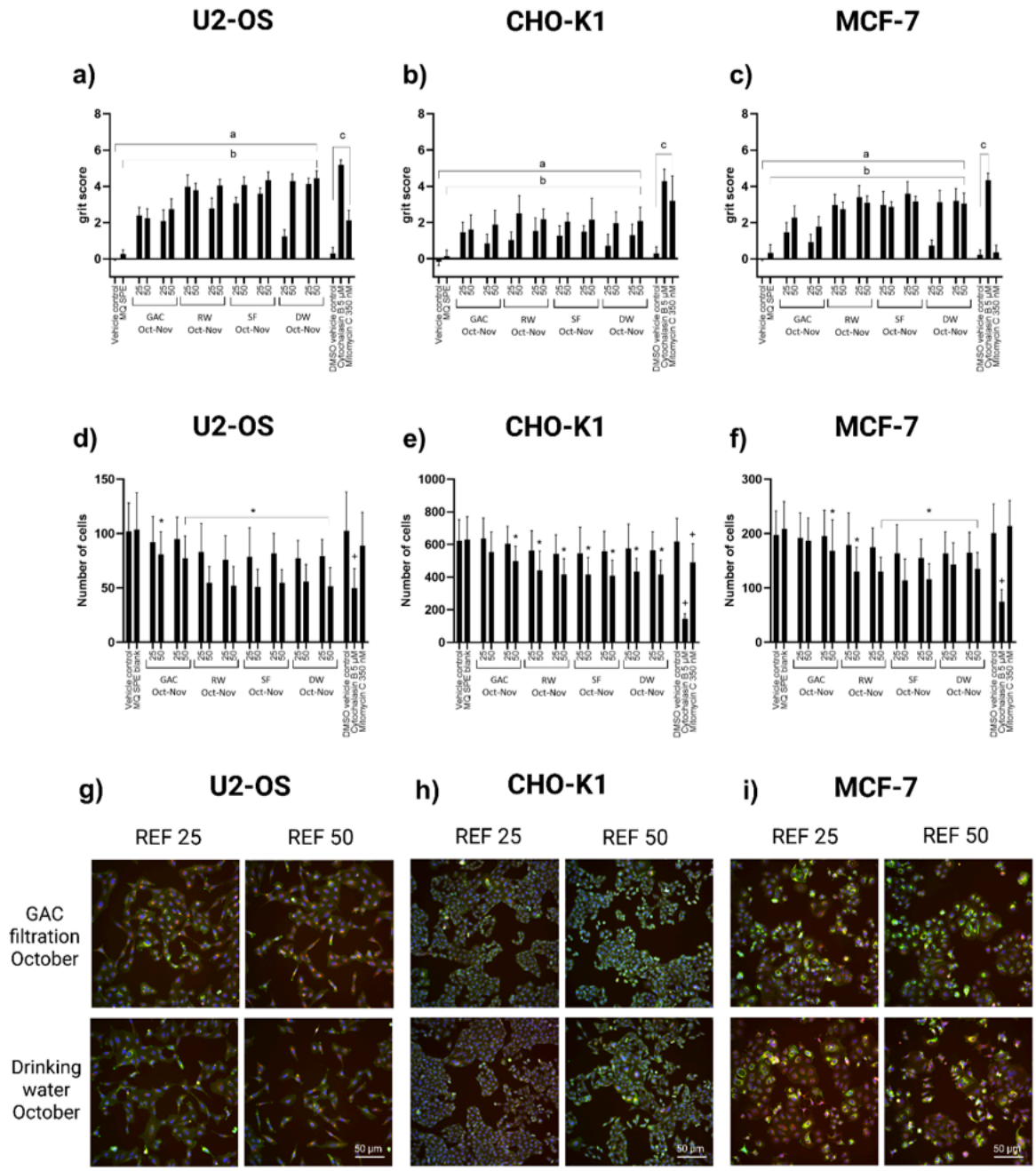


Figure 2

Morphological perturbations and changes in cell count in U2-OS, CHO-K1 and MCF-7 cells exposed to water samples (REFs 25 and 50), MQ SPE, CB (5 µM) and MC (350 nM) for 24 hrs. The upper panels show morphological perturbations in grit scores for **a)** U2-OS, **b)**CHO-K1 and **c)** MCF-7 cells, whereas panels **d)** U2-OS, **e)** CHO-K1 and **f)** MCF-7 show the cell count for all treatments. Water samples were compared against vehicle and MQ SPE controls and reference compounds against DMSO vehicle control using One-way ANOVA and Dunnett's multiple comparison test ($p \leq 0.05$). For grit scores, water samples significantly different from vehicle control are shown as "a" whereas samples significantly different from MQ SPE control are shown as "b" and reference compounds significantly different from DMSO vehicle control are shown as "c". For number of cells, water samples significantly different from vehicle control and MQ SPE control are shown as * and reference compounds significantly different from DMSO vehicle control are shown as +. Data is presented as mean ± SD from technical replicates obtained in a single experiment (3 for each water sample concentration and reference compound and 12 for vehicle and MQ SPE controls). The lower panels show the Cell Painting images of **g)**U2-OS, **h)** CHO-K1 and **i)** MCF-7 cell lines exposed to GAC filtration and drinking water samples at REFs 25 and 50. The images represent merged fluorescence channels of the Hoechst, MitoTracker, Phalloidin/Wheat Germ Agglutinin, SYTO 14, and Concanavalin A staining. Scale bar of all images = 50 µm.

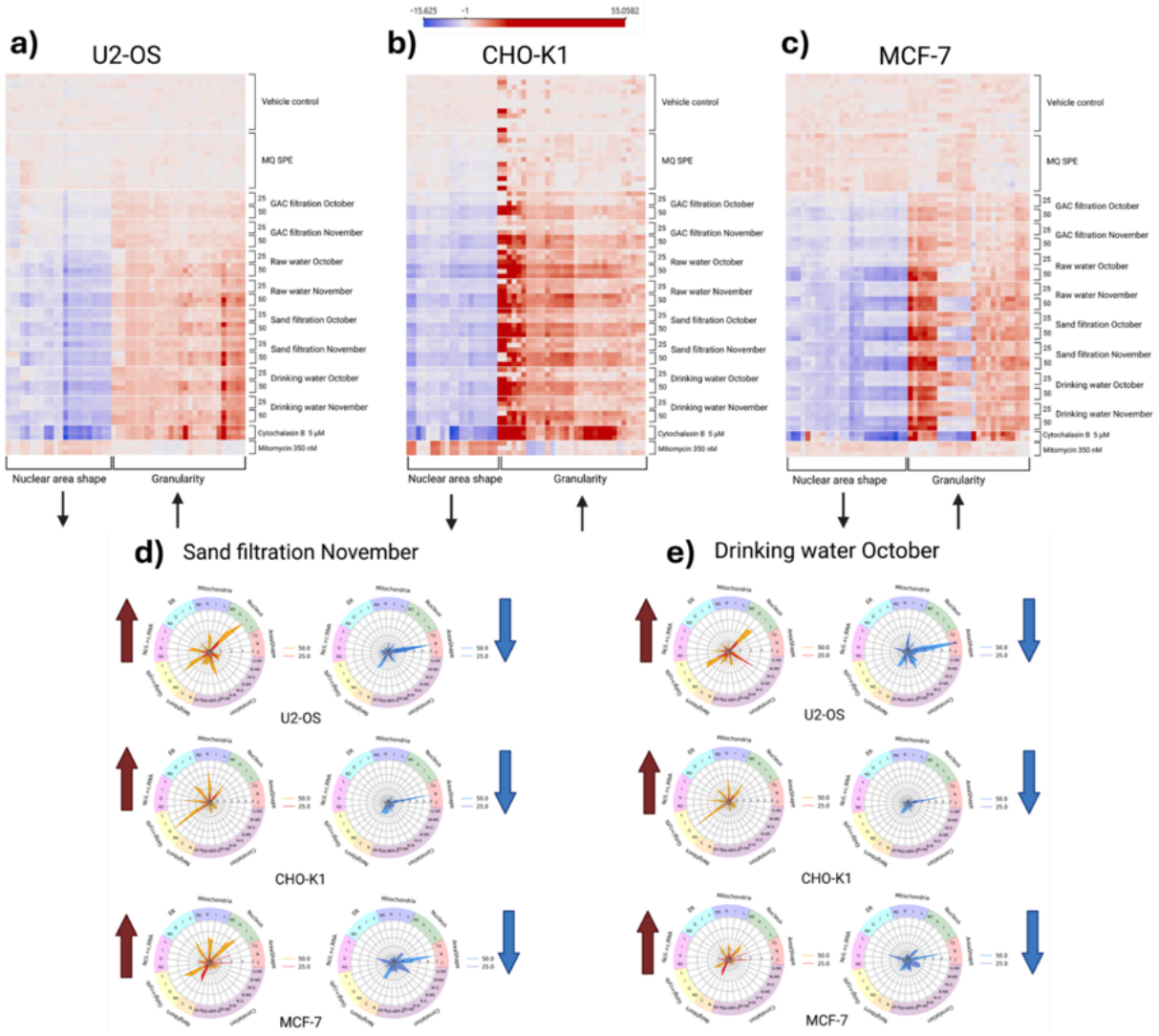


Figure 3

Morphological changes in U2-OS, CHO-K1 and MCF-7 cells exposed to water samples (REFs 25 & 50), MQ SPE, CB (5 µM) and MC (350 nM) for 24 hrs. The upper panels show the heatmaps for changes in the top 50 features for **a)** U2-OS, **b)** CHO-K1 and **c)** MCF-7. The heatmaps display a blue–red color scale, where blue indicates lower values (down to −15.6 - dark blue) and red indicates higher values (up to 55.1 - dark red). The lower panels show examples of the similarities in morphological profiles produced from the changes in the top 50 features between **d)** sand filtration in November and **e)** drinking water in October in the three cell lines. The radar plots summarize morphological features grouped by cellular compartments, including mitochondria, nucleus, actin cytoskeleton, endoplasmic reticulum, Golgi apparatus/plasma membrane, RNA/nucleoli, as well as correlations and neighboring structures. The radar plots with orange-red colors represent high values and blue colors represent low values for features. For all panels, the lower values of features are considered as decrease and are indicated as ↓ and the higher values of features are considered as increase and are indicated as ↑. Heatmaps show the individual profiles of technical replicates obtained in a single experiment (3 for each water sample concentration and reference compound and 12 for vehicle and MQ SPE controls), whereas radar plots display the merged profiles generated from all replicates from the heatmaps.

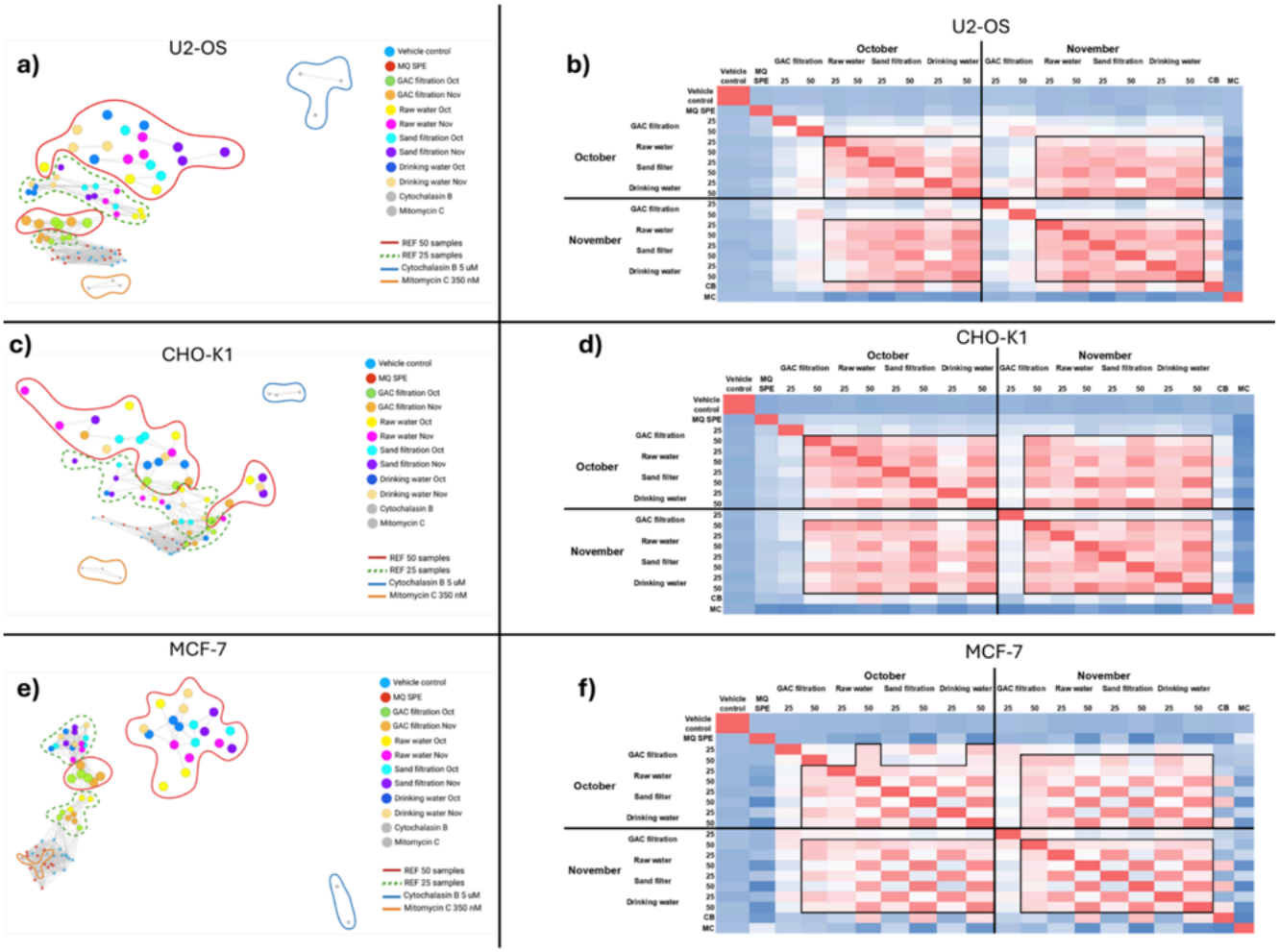


Figure 4

Clustering of and correlations between samples from the treatment steps in U2-OS, CHO-K1 and MCF-7 cells exposed to water samples (REFs 25 & 50), MQ SPE, CB (CB, 5 µM) and MC (MC, 350 nM) for 24 hrs. Panels **a)**, **c)**and **e)** show the morphological similarities across samples in MDS plots. Each datapoint represents the individual morphological profile of each replicate from each treatment. The distance between points reflects the similarity of their profiles, with samples clustering together indicating more similar morphological responses. Datapoints circled in red represent REF50 samples, datapoints circled in a green-dotted line represent REF 25 samples, datapoints circled in blue represent CB and data points circled in orange represent MC. Panels **b)**, **d)** and **f)** show the correlations between water samples in U2-OS, CHO.K1 and MCF-7 cells in October and November. The heatmap displays pairwise correlations between samples based on their phenotypes. The color scale represents the strength and direction of the correlation, with red indicating stronger positive correlations and blue indicating negative or weaker correlations. Correlations between water samples are delimited by a black rectangle. Correlations were calculated between samples based on the data from technical replicates obtained in a single experiment (3 for each water sample concentration and reference compound and 12 for vehicle and MQ SPE controls), with each cell representing the correlation of phenotypes between two samples.

Supplementary Files

This is a list of supplementary files associated with this preprint. Click to download.

- SupplementarymaterialsMechanisticinsights.docx
- Graphicalabstract.docx